ISBN: 978-3-95450-247-9 ISSN: 2673-5490 doi: 10.18429/JACoW-IPAC2024-WEPR12

FIRST COMPARISON STUDIES IN DYNAMIC APERTURE FOR NESTED MAGNETS AND BASELINE LATTICE IN THE FCC-ee

C. García-Jaimes*, T. Pieloni, L. van Riesen-Haupt, M. Seidel, EPFL-LPAP, Lausanne, Switzerland
R. Tomás, CERN, Geneva, Switzerland

Abstract

A significant project such as the FCC-ee (with 91.17 km circumference) entails numerous challenges to ensure the stability and performance of the machine. In the pursuit of contributing to the improvement of energy consumption during its operation, the exploration of Nested Magnets (NMs) as a means to reduce synchrotron radiation has been undertaken. This paper presents first studies on the Dynamic Aperture (DA) and the Momentum Acceptance (MA) of this novel design to guide the next developments.

INTRODUCTION TO DYNAMIC APERTURE AND MOMENTUM ACCEPTANCE

The most important parameters evaluate particle stability in a synchrotron-type accelerator are the DA and the MA. DA is defined as the phase-space volume where particles maintain stable motion over several turns, it requires tracking particles with different initial coordinates in the phase-space [1]. Usually the number of turns chosen for the simulations has to be greater than the longitudinal and transverse damping times. The MA is the maximum momentum deviation to maintain a stable synchrotron motion [2].

The DA and MA are mostly affected by the chromatic properties of the lattice and the required non-linear magnetic components, as sextupoles, present in the lattice for the correction of the natural chromatic aberrations. For this reason an optimization of the sextupolar strengths, k_2, needs to be done in order to maximize the DA and the MA. Occasionally, octupoles are also used in this optimization process, compensating the nonlinear aberrations from sextupoles [3].

Options for the Arrangement of Sextupoles

The first order chromaticity is defined as the derivative of the tune, Q, with respect to the relative momentum deviation as [4]

$$Q' = \frac{dQ}{d\delta}, \quad \delta = \frac{\Delta p_0}{p_0} \tag{1}$$

where δ is the relative momentum deviation and p_0 is the reference momentum. In lepton colliders as the FCC-ee the chromaticity in the absence of sextupoles is large and negative.

The scheme for the global chromaticity correction in the baseline lattices for FCC-ee is a non-interleaved sextupole scheme. This means having sextupole pairs separated by two FODO cells with $2 \times 90°$ phase advance between them, i.e. a phase advance of π [5], This approach offers the most effective reduction of geometric aberrations. For the Z lattice, 75 different families of sextupoles are required, and 145 are needed for tt [6].

With the introduction of NMs in the Z and tt lattices, which feature magnets with independent electric currents capable of exhibiting multiple magnetic component (i.e., dipole + quadrupole + sextupole [7–9]), two possible options for the distribution of sextupoles are considered, as shown in the Fig. 1. The first option involves placing the sextupole component also nested at the nearest quadrupole and scaling k_2 in order to maintain the integrated gradient from the baseline (before matching and optimizing the sextupole families). Consequently, this results in increasing the length of the sextupole from 1.5 m to 2.9 m in the case of Z lattice with this option. For the tt lattice, the sextupole lengths of 3.0 m are converted to 2.9 m.

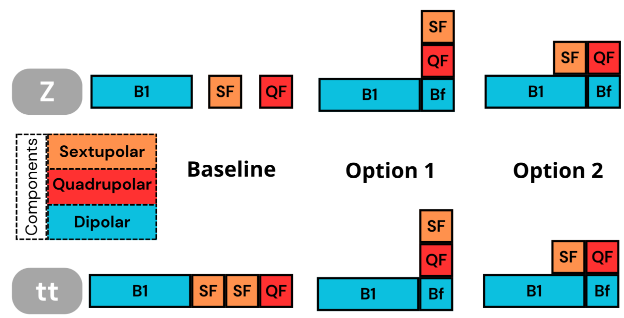

Figure 1: The two options used for studying the dynamic aperture with the implementation of NMs in the FCC-ee. Option 2 is the closest to the baseline (shown on the right of the figure) in terms of optics design. Both options 1 and 2 are feasible according to the magnet design experts.

Option 2 involves maintaining the position and nominal length of the sextupole and adding only a dipole component to make it a NM. This allows for the optics of the NMs lattices to closely resemble that of the baseline. In both NMs options, it is ensured that the phase advance between two consecutive sextupoles is equal to π.

Once the sextupoles were implemented throughout the entire lattice a matching of the Q' is performed in both planes. The results, as well as parameters related to the lattice optics, are shown in detail in Table 1.

Simulation of the DA

For the DA simulation, cpymad [10] and Xsuite [11] were used to track particles in the six available lattices: baseline and the two NMs options for both Z and tt energies.

656 different initial points in the horizontal (Δx) and vertical plane (offset in δ) were used to determine which particles

* cristobal.miguel.garcia.jaimes@cern.ch

15th International Particle Accelerator Conference,Nashville, TN JACoW Publishing
ISBN: 978-3-95450-247-9 ISSN: 2673-5490 doi: 10.18429/JACoW-IPAC2024-WEPR12

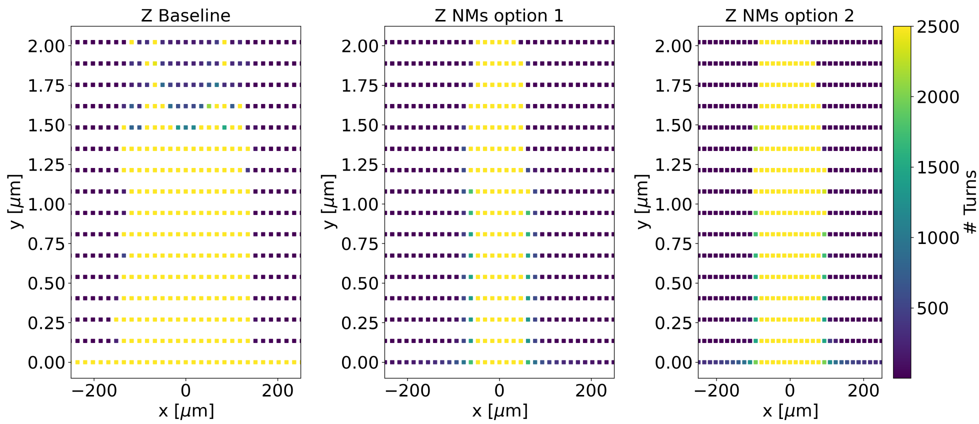

Figure 2: DA for the different lattice options at the Z energy: the baseline and the NMs lattices Options 1 and 2. The plots were obtained with the same number of turns and distribution in the X-Y space for tracking.

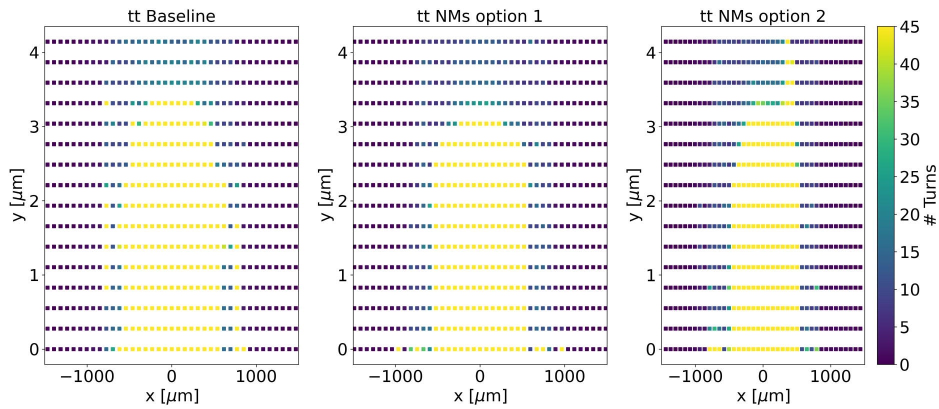

Figure 3: DA in the tt baseline and NMs lattices.

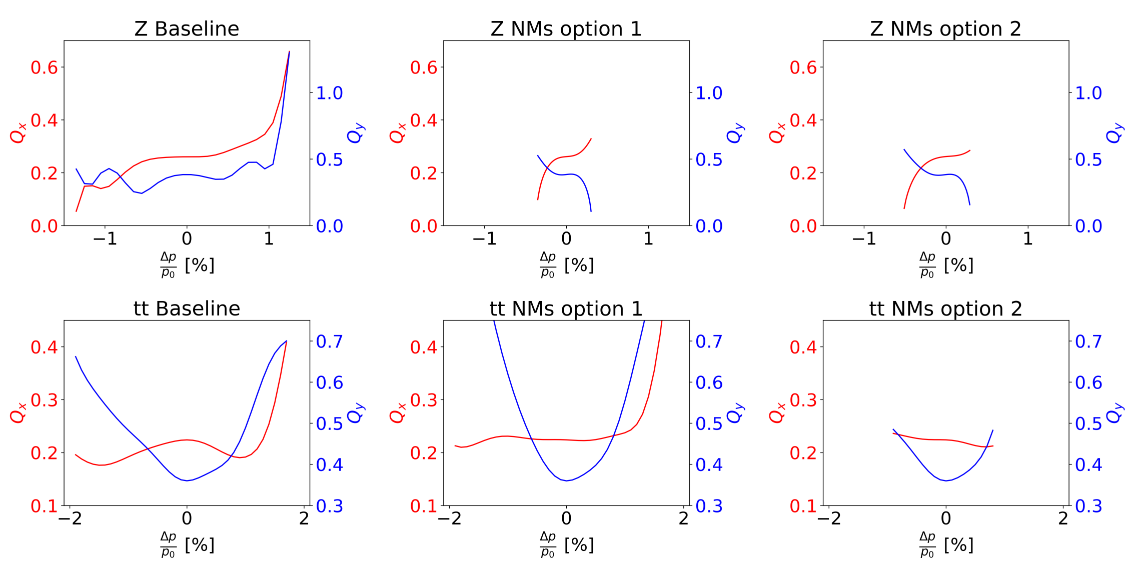

Figure 4: Horizontal and vertical fractional part of tunes versus relative momentum deviation for all the lattices.

ISBN: 978-3-95450-247-9 ISSN: 2673-5490 doi: 10.18429/JACoW-IPAC2024-WEPR12

Table 1: Overview of the different options with sextupoles for the Z and tt lattices with NMs, including optical properties and emittances. The values for ϵ_x and the longitudinal damping time were obtained scaling the energy (10 GeV to 182.5 GeV) using equtions (2) of [8].

	Z baseline	**Option 1**	**Option 2**	**tt baseline**	**Option 1**	**Option 2**
Q_x	214.26	214.26	214.26	402.22	402.22	402.22
Q_y	214.38	214.38	214.38	394.359	394.36	394.36
$Q'_{xnatural}$	-499.30	-505.66	-505.01	-545.15	-545.05	-545.33
$Q'_{ynatural}$	-3223.59	-3231.71	-3175.24	-2061.67	-2065.94	-2066.53
Q'_x	0.081	2.43	2.544	0.021	-0.52	-0.47
Q'_y	-0.007	6.39	6.53	0.010	-0.19	-0.16
# Families of Sextupoles	75	75	75	146	146	146
Δk_2 SF	0	-8.81 %	-2.51 %	0	-17.98%	+2.95%
ΔK_2 SD	0	-17.90%	-15.86 %	0	-7.32%	+5.43%
ϵ_x [nm]	0.705	0.605	0.605	1.47	1.38	1.29
Long. damping time [turns]	1167	1385	1385	18	21	22

survive during the tracking with mean radiation. The total number of turns to carry out the simulations is approximately twice the longitudinal damping time and the ϵ_y is obtained from [12].

PRELIMINARY DA AND MA RESULTS

The data obtained from the tracking is shown in Figs. 2 and 3. For the Z energy it is observed that the dynamic aperture of both alternative options decreases in the horizontal direction and increases vertically. Differently, for the tt lattice, the Option 1 features very similar DA to the baseline performance, while this is not the case for Option 2 that shows a reduction.

By using the Twiss module in MADX [13], various simulations are performed to obtain the momentum acceptance range for each lattice option. These calculations were carried out without radiation. Figure 4 illustrates the fluctuation of the fractional part of the horizontal and vertical tunes, Q_x and Q_y, as a function of δ, both for the Z and tt lattices. The tt NMs lattices feature similar MA to the baseline, being Option 1 the closest to the baseline. However, both Z NMs options clearly feature a significantly reduced MA compared to the baseline due to a cubic component of the tunes versus δ in this first study.

CONCLUSION AND OUTLOOK

First DA and MA calculations have been performed for two NMs lattice configurations for the Z and tt energies. For the tt case very promising results are obtained with DA and MA being close to the baseline. However, for the Z energy the horizontal DA and the MA are significantly reduced. Further optics optimizations must be carried out for the Z NMs lattices in order to achieve performances closer to the baseline.

ACKNOWLEDGEMENTS

This study is supported by the Swiss Accelerator Research and Technology (CHART). This project has received funding from the European Union's Horizon 2020 research and innovation programme under the Marie Skłodowska-Curie grant agreement No. 945363, EPFLglobaLeaders.

REFERENCES

[1] S. Turner *et al.* (eds.), "CAS - CERN Accelerator School Fourth General Accelerator Physics Course", *Proceedings*, p. 58, 1991. https://inis.iaea.org/collection/NCLCollectionStore/_Public/23/001/23001782.pdf

[2] H. Wiedemann, "Particle accelerator physics", 4th ed. , Springer, 2015. doi:10.1007/978-3-319-18317-6

[3] J. Zhang *et al.*, "Increasing the Dynamic and Momentum Apertures of the ThomX Ring by Means of Octupole Correctors", in *Proc. IPAC'15*, Richmond, VA, USA, May 2015, pp. 121–124. doi:10.18429/JACoW-IPAC2015-MOPWA016

[4] S. Guiducci, "Chromaticity, CAS - CERN Accelerator School : 5th General Accelerator Physics Course", pp. 191–206. doi:10.5170/CERN-1994-001.191

[5] B. Haerer and T. Tydecks, "Lattice Design and Dynamic Aperture Studies for the FCC-ee Top-Up Booster Synchrotron", 2021. doi:10.48550/arXiv.2111.14462

[6] M. Benedikt *et al.* (eds.), "FCC-ee: The Lepton Collider: Future Circular Collider Conceptual Design Report Volume 2", *The European Physical Journal Special Topics*, vol. 228,

ISBN: 978-3-95450-247-9 ISSN: 2673-5490 doi: 10.18429/JACoW-IPAC2024-WEPR12

no. 2, pp. 261–623, Jun. 2019.
doi:10.1140/epjst/e2019-900045-4

[7] C. García-Jaimes, T. Pieloni, L. Riesen-Haupt, M. Seidel and R. Tomas, "Exploring FCC-ee Optics Designs with Combined Function Magnets", *J. Phys. Conf. Ser.*, vol. 2687, no. 2, p. 022007, Jan. 2024.
doi:10.1088/1742-6596/2687/2/022007

[8] C. García-Jaimes, T. Pieloni, L. Riesen-Haupt, M. Seidel, and R. Tomas, "First FCC-ee lattice designs with Nested Magnets", presented at the IPAC'24, Nashville, TN, USA, May 2024, paper WEPR10, this conference.

[9] C. M. Garcia Jaimes *et al.*, "Parameter space for the magnetic design of Nested Magnets in the FCC-ee arc cell", presented at the IPAC'24, Nashville, TN, USA, May 2024, paper WEPR11, this conference.

[10] T. Gläßle, CERN, (26.04.2024). https://github.com/hibtc/cpymad

[11] G. Iadarola *et al.*, "Xsuite: An Integrated Beam Physics Simulation Framework", in *Proc. HB'23*, Geneva, Switzerland, Oct. 2024, pp. 73–80.
doi:10.18429/JACoW-HB2023-TUA2I1

[12] K. Oide, "Polarimeter and wigglers integration status", FCC WEEK2022, (01.06.2022), p. 3, https://indico.cern.ch/event/1064327/contributions/4893299/attachments/2452194/4204014/Polmeter_Wiggler_Oide_220601.pdf

[13] CERN, (04.12.2023). https://madx.web.cern.ch/madx